J|A|C|S
ARTICLES
Published on Web 09/22/2006

Effects of the Alternating Backbone Configuration on the Secondary Structure and Self-Assembly of β-Peptides

Tamás A. Martinek,† István M. Mándity,† Lívia Fülöp,‡ Gábor K. Tóth,‡ Elemér Vass,§ Miklós Hollósi,§ Eniko Forró,† and Ferenc Fülöp*,†

Contribution from the Institute of Pharmaceutical Chemistry and Department of Medical Chemistry, University of Szeged, H-6701 Szeged, POB 427, Hungary, and Institute of Chemistry, Department of Organic Chemistry, Eötvös Loránd University, Pázmány P. s. 1/A, H-1117 Budapest, Hungary

Received June 3, 2006; E-mail: fulop@pharm.u-szeged.hu

Abstract: Heterochiral homo-oligomers with alternating backbone configurations were constructed by using the different enantiomers of the *cis*- and *trans*-2-aminocyclopentanecarboxylic acid (ACPC) monomers. Molecular modeling and the spectroscopic techniques (NMR, ECD, and VCD) unequivocally proved that the alternating heterochiral *cis*-ACPC sequences form an H10/12 helix, where extra stabilization can be achieved via the cyclic side chains. The ECD and TEM measurements, together with molecular modeling, revealed that the alternating heterochiral *trans*-ACPC oligomers tend to attain a polar-strand secondary structure in solution, which can self-assemble into nanostructured fibrils. The observations indicate that coverage of all the possible secondary structures (various helix types and strand-mimicking conformations) can be attained with the help of cyclic β-amino acid diastereomers. A relationship has been established between the backbone chirality pattern and the prevailing secondary structure, which underlines the role of stereochemical control in the β-peptide secondary structure design and may contribute to future biological applications.

Introduction

The β-peptide foldamers belong among the most intriguing models of unnatural polymers[1] as they are able to form secondary structures (various helix-types, strand-like conformations, and turns) and are capable of forming higher-order self-assemblies too.[2] The importance of these molecules in chemistry and biochemistry is justified by the following facts. First, β-peptide oligomers with a designed molecular interaction field have gained several biological applications, for example, as inhibitors of fat and cholesterol absorption,[3] selective antibacterial amphiphiles,[4] RNA-binding foldamers,[5] inhibitors of the interaction between the tumor suppressor p53 and the sequestering factor hDM2,[6] rationally designed antiviral substances,[7] and T−N antigen-conveying helix.[8] On the other hand, the secondary structure patterns available to β-peptides are efficiently controlable via the side-chain chemistry and especially via the backbone configurations, and the tailored self-assembly of the secondary structure units was recently observed.[2] The principles of the β-peptide foldamer design have been discussed extensively,[9] and these rules have been established mainly for uniformly substituted β-amino acids with respect both to the side-chain position (β^3 and/or β^2) and to the backbone stereochemistry. Noteworthy exceptions are the β^2/β^3 sequences of Seebach et al., which basically introduced the alternating design approach to the field. These oligomers not only formed the stable alternating H10/12 helices that are unique to the β-peptides,[10] but also acquired importance from the aspect of medicinal

† Institute of Pharmaceutical Chemistry, University of Szeged.
‡ Department of Medical Chemistry, University of Szeged.
§ Eötvös Loránd University.

(1) (a) Garric, J.; Léger, J.-M.; Huc, I. *Angew. Chem., Int. Ed.* **2005**, *117*, 1990−1994. (b) Farrera-Sinfreu, J.; Zaccaro, L.; Vidal, D.; Salvatella, X.; Giralt, E.; Pons, M.; Albericio, F.; Royo, M. *J. Am. Chem. Soc.* **2004**, *126*, 6048−6057. (c) Tie, C.; Gallucci, J. C.; Parquette, J. R.; *J. Am. Chem. Soc.* **2006**, *128*, 1162−1171. (d) Gellman, S. H. *Acc. Chem. Res.* **1998**, *31*, 173−180. (e) Sanford, A. R.; Yamato, K.; Yang, X.; Yuan, L.; Han, Y.; Gong, B. *Eur. J. Biochem.* **2004**, *271*, 1416−1425.

(2) (a) Martinek, T. A.; Hetényi, A.; Fülöp, L.; Mándity, I. M.; Tóth, G. K.; Dékány, I.; Fülöp, F. *Angew. Chem., Int. Ed.* **2006**, *45*, 2396−2400. (b) Yang, Z. M.; Liang, G. L.; Xu, B. *Chem. Commun.* **2006**, 738−740. (c) Raguse, T. L.; Lai, J. R.; LePlae, P. R.; Gellman, S. H. *Org. Lett.* **2001**, *3*, 3963−3966. (d) Cheng, R. P.; DeGrado, W. F. *J. Am. Chem. Soc.* **2001**, *124*, 11564−11565. (e) Hetényi, A.; Mándity, I. M.; Martinek, T. A.; Tóth, G. K.; Fülöp, F. *J. Am. Chem. Soc.* **2005**, *127*, 547−553. (f) Chakraborty, P.; Diederichsen, U. *Chem. Eur. J.* **2005**, *11*, 3207−3216.

(3) Werder, M.; Hauser, H.; Abele, S.; Seebach, D. *Helv. Chim. Acta* **1999**, *82*, 1774−1783.

(4) Porter, E. A.; Wang, X.; Lee, H.; Weisblum B.; Gellman, S. H. *Nature* **2000**, *404*, 565−565.

(5) Gellman, M. A.; Richter, S.; Cao, H.; Umezawa, N.; Gellman, S. H.; Rana, T. M. *Org. Lett.*, **2003**, *5*, 3563−3565.

(6) Kritzer, J.A.; Stephens, O. M.; Guarracino, D. A.; Reznik, S. K.; Schepartz, A. *Bioorg. Med. Chem.* **2005**, *13*, 11−16.

(7) English, E. P.; Chumanov, R. S.; Gellman, S. H.; Compton, T. *J. Biol. Chem.* **2006**, *281*, 2661−2667.

(8) Norgren, A. S.; Arvidsson, P. I. *Org. Biomol. Chem.* **2005**, *3*, 1359−1361.

(9) (a) Cheng, R. P.; Gellman, S. H.; DeGrado, W. F. *Chem. Rev.* **2001**, *101*, 3219−3232. (b) Seebach, D.; Beck, A. K.; Bierbaum, D. J. *Chem. Biodiversity* **2004**, *1*, 1111−1239. (c) Martinek, T. A.; Fülöp, F. *Eur. J. Biochem.* **2003**, *270*, 3657−3666. (d) Cheng, R. P. *Curr. Opin. Struct. Biol.* **2004**, *14*, 512−520.

(10) (a) Seebach, D.; Gademann, K.; Schreiber, J. V.; Matthews, J. L.; Hintermann, T.; Jaun, B. *Helv. Chim. Acta* **1997**, *80*, 2033−2038. (b) Seebach, D.; Abele, S.; Gademann, K.; Guichard, G.; Hintermann, T.; Jaun, B.; Matthews, J. L.; Schreiber, J. V. *Helv. Chim. Acta* **1998**, *81*, 932−982. (c) Rueping, M.; Schreiber, J. V.; Lelais, G.; Jaun, B.; Seebach, D. *Helv. Chim. Acta* **2002**, *85*, 2577−2593. (d) Seebach, D.; Mathad, R. I.; Kimmerlin, T.; Mahajan, Y. R.; Bindschädler, P.; Rueping, M.; Jaun, B.; Hilty, C.; Etezady-Esfarjani, T. *Helv. Chim. Acta* **2005**, *88*, 1969−1982.

Scheme 1. The Studied Alternating Heterochiral β-Peptide Sequences[a]

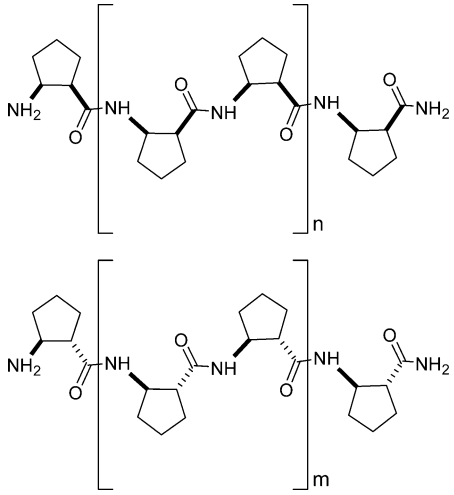

[a] **1**, $n = 1$; **2**, $n = 2$; **3**, $m = 1$, **4**, $m = 2$.

chemistry.[11] The alternating design principle was recently successfully extended to the combined α/β-peptides, which showed signs of a propensity to fold for short sequences.[12]

In the present work, we make an attempt to extend the concept of alternating sequences further by combining it with stereochemical control over the secondary structure and with the approach of stabilization by cyclic side chains. We demonstrate that both stable H10/12 helices and self-assembling polar strands can be constructed by designing alternating heterochiral sequences with the incorporation of cyclic β-amino acid residues.

Results and Discussion

The homochiral homo-oligomers of the *trans*-ACPC (*trans*-1*R*,2*R*-aminocyclopentanecarboxylic acid) are known to form H12 helices,[13] while *cis*-ACPC residues (*cis*-1*R*,2*S*-aminocyclopentanecarboxylic acid) or the *cis*-β-norbornene amino acids facilitate the strand-mimicking structure.[14] To test the potential of the alternating heterochiral approach, we chose ACPC monomers, because all four diastereomers are available synthetically in a reasonably convenient way for this β-residue.[15] Both alternating heterochiral *cis*-ACPC (H-[(1*S*,2*R*)-ACPC-(1*R*,2*S*)-ACPC]$_n$-NH_2) and heterochiral *trans*-ACPC (H-[(1*S*,2*S*)-ACPC-(1*R*,2*R*)-ACPC]$_m$-NH_2) oligomers were constructed (Scheme 1).

In the first step, molecular modeling was perfomed for hexamers **2** and **4** at the force-field and ab initio quantum mechanical levels. A standard simulated annealing conformational search protocol was carried out by using molecular mechanics without any distance restraint. The resulting conformational ensembles were analyzed, and the representative conformers from the lowest-energy conformational families of **2** and **4** were selected and further optimized. For the ab initio quantum chemical geometry optimizations,[16] the HF/3-21G level of theory in a vacuum was utilized first, as this has been reported to provide a good approximation for the geometry of the β-peptides.[17] The structures converged to the corresponding local minimum of the potential energy surface. To take into account the effects of more diffuse basis sets and the electron correlation, the optimizations were performed at the B3LYP/6-311G** level too (Figure 1).

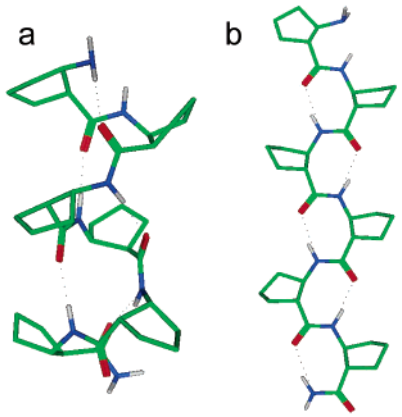

Figure 1. Ab initio geometries of **2** (a) and **4** (b), calculated for the isolated molecules in a vacuum.

For **2**, the conformational search and the final optimization performed on the isolated molecules clearly predicted the H10/12 helix as the prevailing structure. At the same time, the H8 strandlike conformation was the most stable for **4**. Since our earlier results on the strand-mimicking β-peptide oligomers revealed their tendency toward self-assembling,[2a] we modeled the possibility of interstrand interactions for **4**. Starting geometries for parallel and antiparallel sheetlike dimers of the polar strands were built by using molecular mechanics, and these larger systems were optimized by using the force-field combined with implicit solvent model. Both the parallel and the antiparallel arrangement resulted in stable dimers where the interstrand H-bonds are ideally positioned and there is no steric repulsion between the side-chains (Figure 2). These findings render self-association into a fibrillar morphology likely.

On the basis of the promising modeling results, model compounds **1**−**4** were synthesized. The four Boc-ACPC diastereomers were prepared by using literature methods.[15] The chain assembly was carried out on a solid support, with Boc chemistry and DCC/HOBt coupling. In the case of **4**, difficulties arose during the fifth and the sixth coupling steps, which led to decreased yields. The peptides were detached from the resin by using liquid HF, and the products were isolated by RP-HPLC. The final products were characterized by means of MS and various NMR methods, including COSY, TOCSY, and ROESY, in 4 mM CD_3OD, DMSO, and water (90% H_2O + 10% D_2O) solutions. The NMR signal dispersions were very good for **1**

(11) Arvidson, P. I.; Ryder, N. S.; Weiss, H. M.; Gross, G.; Kretz, O.; Woessner, R.; Seebach, D. *ChemBioChem*, **2003**, 4, 1345−1347.
(12) (a) De Pol, S.; Zorn, C.; Klein, C. D.; Zerbe, O.; Reiser, O. *Angew. Chem., Int. Ed.* **2004**, *43*, 511−514. (b) Hayen, A.; Schmitt, M. A.; Ngassa, F. N.; Thomasson, K. A.; Gellman, S. H. *Angew. Chem., Int. Ed.* **2004**, *43*, 505−510. (c) Roy, R. S.; Karle, I. L.; Raghothama, S.; Balaram, P. *Proc. Natl. Acad. Sci. U.S.A.* **2004**, *101*, 16478−16482. (d) Schmitt, M. A.; Choi, S. H.; Guzei, I. A.; Gellman, S. H. *J. Am. Chem. Soc.* **2005**, *127*, 13130−13131.
(13) Appella, D. H.; Christianson, L. A.; Klein, D. A.; Powell, D. R.; Huang, X. L.; Barchi, J. J.; Gellman, S. H. *Nature* **1997**, *387*, 381−384.
(14) (a) Martinek, T. A.; Tóth, G. K.; Vass, E.; Hollósi, M.; Fülöp, F. *Angew. Chem., Int. Ed.* **2002**, *41*, 1718−1721. (b) Chandrasekhar, S.; Babu, B. N.; Prabhakar, A.; Sudhakar, A.; Reddy, M. S.; Kiran, M. U.; Jagadeesh, B. *Chem. Commun.* **2006**, 1548−1550.
(15) (a) LePlae, P. R.; Umezawa, N.; Lee, H. S.; Gellman, S. H. *J. Org. Chem.* **2001**, *66*, 5629−5632. (b) Forró, E.; Fülöp F. *Org. Lett.* **2003**, *5*, 1209−1212. (c) Forró, E.; Fülöp F. *Mini-Rev. Org. Chem.* **2004**, *1*, 93−102.
(16) Frisch, M. J.; et al. *Gaussian 03*, revision A.1; Gaussian, Inc.: Pittsburgh, PA, 2003; http://www.Gaussian.com.
(17) (a) Beke, T.; Csizmadia, I. G.; Perczel, A. *J. Comput. Chem.* **2004**, *25*, 285−307. (b) Mohle, K.; Gunther, R.; Thormann, M.; Sewald, N.; Hofmann, H. J. *Biopolymers* **1999**, *50*, 167−184.

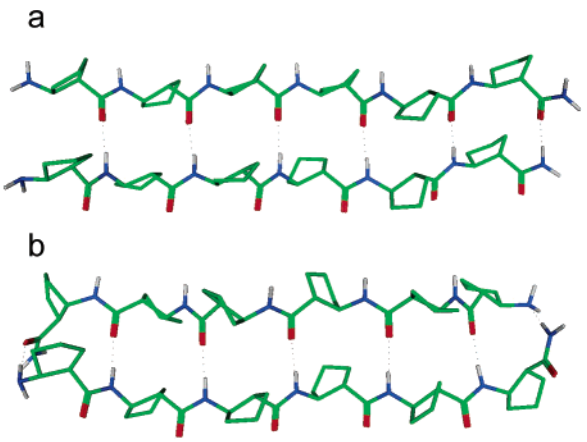

Figure 2. Geometry for the parallel (a) and antiparallel (b) sheet fragments of **4**, calculated by means of molecular mechanics (MMFF94 with implicit water).

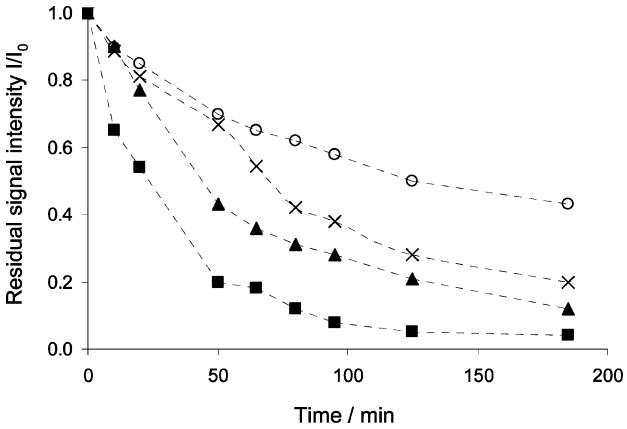

Figure 3. Time dependence of the NH/ND exchange for **2** in CD_3OD: ○, NH_3; ▲, NH_4; ■, NH_5; ×, NH_6.

and **2**, and thus the resonance assignment was achievable along the backbone. As concerns the aggregation of these compounds, neither the resonance broadening nor the diffusion NMR data indicated increased particle size. Vibrational circular dichroism (VCD) has become a powerful technique with which to study the stereochemical and conformational features of the molecules,[18] and it was utilized in this work too. Its advantages are that VCD spectra have a rich structural content and, by comparison of the ab initio calculated VCD spectra with the experimental one, the structural hypothesis can be evaluated directly. Unfortunately, **3** and **4** exhibited extremely low resonance dispersion, preventing any high-resolution structure determination by NMR. Moreover, the solubility of **4** was limited, preventing VCD measurements where higher concentration is necessary. Nevertheless, the electronic circular dichroism (ECD) and transmission electron microscope (TEM) images furnished highly informative results.

For assessment of the conformational stability of the peptides **1** and **2** in CD_3OD, N^1H-N^2D exchange was utilized. The time dependence of the residual NH signal intensities of **2** points to the corresponding atoms are considerably shielded from the solvent, because of H-bonding interactions (Figure 3). The proton resonances belonging to terminal nitrogen, amide NH_2, and the C-terminal amide disappeared immediately after dissolution, while the other signals remained for a longer period of time. The exchange pattern observed is in good accord with the theoretically predicted H10/12 helix. For **1**, a similar exchange pattern was detected, but the exchange rates were significantly higher, suggesting a less-ordered structure.

To prove the helical fold of **2**, ROESY experiments were run in CD_3OH, DMSO-d_6, and water (90% H_2O + 10% D_2O). In CD_3OH and DMSO-d_6, the characteristic $C^{\beta}H_2-NH_4$, $NH_3-C^{\beta}H_5$ and $C^{\beta}H_4-NH_6$ long-range NOE interactions could readily be observed, which unambiguously prove the predominant H10/12 helical conformation (Figure 4). For alternating peptide bond orientations and a helix conformation, the neighboring amide protons can be in proximity to each other. Accordingly, ROESY cross-peaks were detected for NH_3-NH_4 and NH_5-NH_6, which is further evidence in support of the H10/12 helix.

Importantly, the $C^{\beta}H-NH$ vicinal couplings exhibited an alternating pattern (values given for DMSO): 9.8 Hz for $NH_3-C^{\beta}H_3$ and $NH_5-C^{\beta}H_5$, and 7.8 Hz for $NH_2-C^{\beta}H_2$, $NH_4-C^{\beta}H_4$ and $NH_6-C^{\beta}H_6$. These ^3J values are in line with the ab initio H10/12 conformation. For **1**, only a weak $C^{\beta}H_2-NH_4$ NOE cross-peak was detected. In aqueous medium, these important cross-peaks and the alternating coupling constant pattern did not appear. These observations point to the stability of the newly designed H10/12 helix, even in the chaotropic solvent DMSO, but the structure is still sensitive to water.

Because of the heterochiral nature of the studied H10/12 models, the arrangement of the backbone hydrogens does not allow the observation of any further $C^{\beta}H-C^{\alpha}H$, $C^{\beta}H-C^{\beta}H$, or $C^{\alpha}H-C^{\alpha}H$ NOE interactions. Electronic and vibrational CD measurements were carried out to gain further supporting evidence for the presence of the H10/12 helix. Unfortunately, the ECD spectra in DMSO are not useful for secondary structural analysis of peptides and proteins, owing to interfering absorption from the solvent below 268 nm. The ECD measurements in methanol revealed a positive Cotton effect, with the positive band at around 210 nm and the negative band at around 190 nm for both **1** and **2** (Figure 5a). However, the intensity of the Cotton effect was markedly lower for **1**. These findings corroborate our conclusions concerning the helically ordered structure in organic solvents. In water, the ECD curves (Figure 5b) displayed Cotton effects, but their intensities were considerably lower as compared with the ECD data in methanol. The relatively increased negative band at 190 nm for **1** indicates the presence of a more elongated conformation. Our H10/12 helix model with purely hydrophobic side-chains still exhibits some helical content in aqueous medium, but the structure is only partially ordered in consequence of the absence of additional stabilizing electrostatic interactions.[19] To complement the solution-phase structure analysis, **2** was characterized by using VCD in the H-bond-breaking DMSO and the strongly H-bond-promoting dichloromethane (DCM) (Figure 6). The recorded curves show intense rotatory strengths in the amide I and II regions of the vibrational spectrum in both solvents. Moreover, the theoretically calculated VCD spectrum based on

(18) (a) Freedman, T. B.; Cao, X.; Dukor, R. K.; Nafie, L. A. *Chirality* **2003**, *15*, 743−758. (b) Keiderling, T. A. In *Circular Dichroism and the Conformational Analysis of Biomolecules;* Fasman, G. D., Ed.; Plenum: New York, 1996; pp 555−598. (c) Stephens, P. J.; Devlin, F. J. *Chirality* **2000**, *12*, 172−179.

(19) Hart, S. A.; Bahadoor, A. B. F.; Matthews, E. E.; Qiu, X. J.; Schepartz, A. *J. Am. Chem. Soc.* **2002**, *125*, 4022−4023

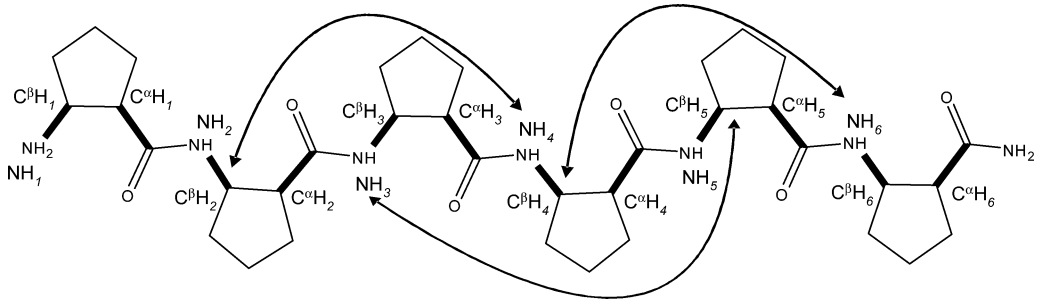

Figure 4. Long-range NOE interactions observed for **2**.

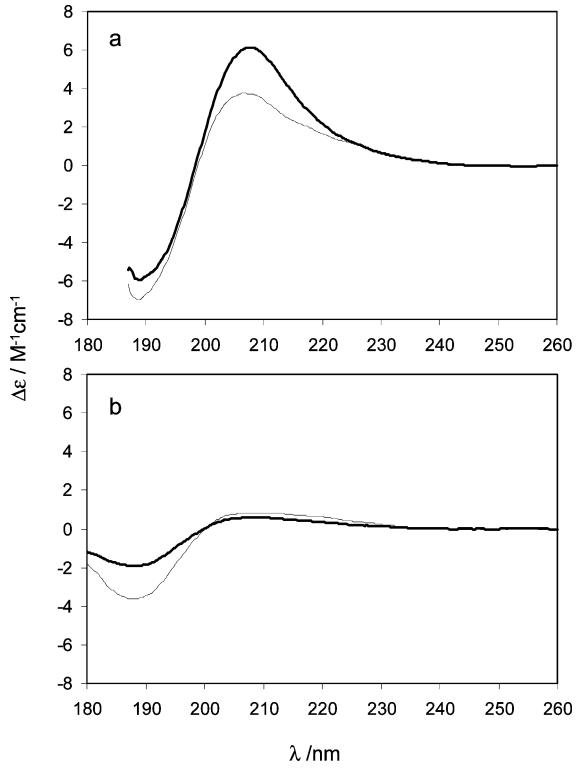

Figure 5. ECD results for **1** (thin curve) and **2** (thick curve) measured in methanol (a) and in water (b), normalized to chromophore units.

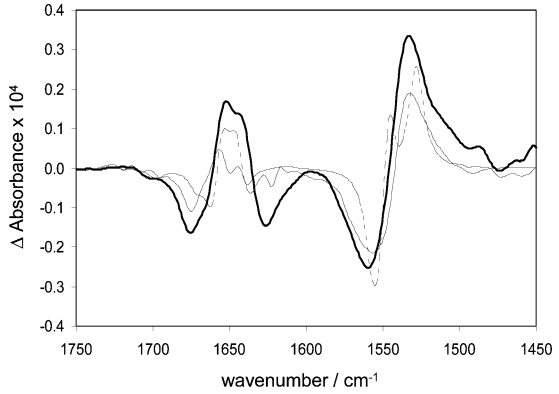

Figure 6. VCD curves for **2**, measured in DCM (thick continuous line), in DMSO (thin continuous line), and the calculated results (dashed, given in scaled VCD units).

the H10/12 ab initio model (see Figure 1a) is in very good agreement with the experimental data with respect to both the frequencies and the signs of the rotatory strengths, which not only proves the helical fold, but also gives information on the absolute direction of the helicity. The VCD results in DMSO

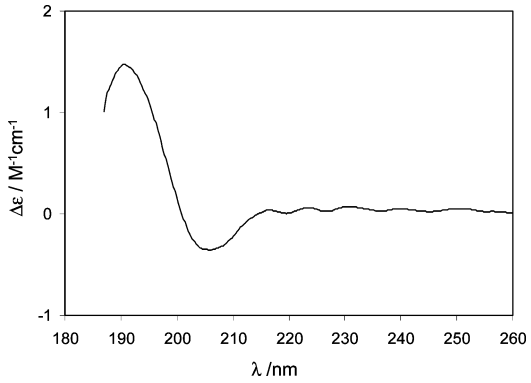

Figure 7. ECD results for **4**, measured in methanol at a concentration of 1 mM, normalized to chromophore units.

corroborate that the H10/12 helix with cyclic side chains remains stable even in the H-bond-breaking solvent.

As mentioned above, NMR measurements were not useful for **3** and **4** because of the signal dispersion problems. However, the absence of the well-resolved NMR signals does not automatically rule out the possibility of an ordered secondary structure. ECD measurements were run and **4** furnished a reasonably intense negative Cotton effect (Figure 7), which suggests the presence of a periodic secondary structure. The negative band appeared at around 205 nm with decreased relative intensity, and the positive band was detected at around 190 nm. These features makes the ECD curve similar to that obtained for the homochiral *cis*-ACPC$_n$ strands (taking into account the absolute configuration).[14a]

Since the modeling results suggested the possibility of infinite sheet formation in the case of **4**, TEM images were recorded to test any fibrillar morphology in solution. The samples were prepared in methanol and water at a concentration of 4 mM. One day after dissolution, no specific morphology was observed. After incubation for one week in water at room temperature, the TEM images exhibited fibrils for **4**, with an average width of 6 nm and a length in the μm range (Figure 8). The fibrils displayed uniform helical twists, with a periodicity of 60 nm. In methanol, certain aggregated objects were observed for **4**, but the fibrillar morphology could not be recognized. Self-assembly was not detected for **3** at all. In view of the literature data that have accumulated on the fibril-forming peptides,[20] and

(20) (a) Sunde, M.; Serpell, L. C.; Bartlam, M.; Fraser, P. E.; Pepys, M. B.; Blake, C. C. F. *J. Mol. Biol.* **1997**, *273*, 729−739. (b) Malinchik, S. B.; Inouye, H.; Szumowski, K. E.; Kirschner, D. A. *Biophys. J.* **1998**, *74*, 537−545. (c) Lamm, M. S.; Rajagopal, K.; Schneider, J. P.; Pochan, D. J. *J. Am. Chem. Soc.* **2005**, *127*, 16692−16700. (d) Fülöp, L.; Zarándi, M.; Datki, Z.; Soós, K.; Penke, B. *Biochem. Biophys. Res. Commun.* **2004**, *324*, 64−69. (e) West, M. W.; Wang, W.; Patterson, J.; Mancias, J. D.; Beasley, J. R.; Hecht, M. H. *Proc. Natl. Acad. Sci. U.S.A.* **1999**, *96*, 11211−11216.

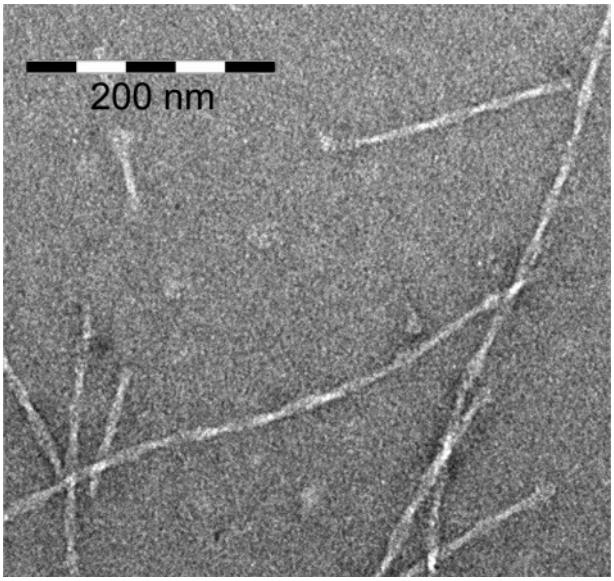

Figure 8. TEM image of **4** measured in water after one week of incubation.

of our earlier results on the self-assembly of homochiral *cis*-ACPC$_n$ strands into nanoribbons, the TEM observations presented here strongly suggest that the preferred secondary structure of **4** is the polar strand, which tends to self-assemble into infinite sheet sandwiches. The self-association appears to be chain-length dependent, since **3** did not show any sign of self-assembly.

Conclusions

β-Peptides with alternating sequences, constructed either by using a nonuniform substitution pattern (β^2/β^3) or with a combination of α- and β-residues, proved very useful in foldamer design and in terms of potential biological applications. The extension of the alternating sequence approach to the heterochiral chains offers a new way to cover the space of periodic folded β-peptide conformations. The modeling results predicted an H10/12 helix for the alternating heterochiral *cis*-ACPC oligomers (**1** and **2**), whereas the *trans*-ACPC counterpart (**3** and **4**) exhibited a propensity to attain a strand-mimicking conformation. For **1** and **2**, the high-resolution 3D assignment made by using NMR, ECD, and VCD unequivocally proved the prevailing H10/12 secondary structure in organic solvents. The results support the view that the helix stability is chain length-dependent, as **2** displayed increased order. Importantly, a stable helical fold was observed even in the chaotropic DMSO, which suggests increased stability following the incorporation of the cyclic side-chains. The ECD results indicated a residual helical content in water, though the spectroscopic results revealed that the studied oligomers are still sensitive to the aqueous medium. In the cases of **3** and **4**, the high-resolution structural characterization could not be achieved, but the ECD observations clearly pointed to a periodically ordered secondary structure in solution for **4**. The preferred polar-strand conformation is supported by the fact that the self-assembly of **4** into nanostructured fibrils was observed in water. According to the literature, this is an unambiguous sign of the presence of the infinite strand-sheet sandwiches organized by the interstrand H-bonds and solvent-driven hydrophobic interactions between the side chains. The self-assembly was chain-length dependent, since tetramer **3** did not exhibit self-association.

It can be concluded that the combination of cyclic β-amino acid residues with alternating backbone configurations is an efficient tool with which to construct helical and strand-mimicking secondary structures. While homochiral *trans*-ACPC homoligomers form an H12 helix,[4] the alternating heterochiral *trans*-ACPC sequence leads to a polar strand. Our earlier results revealed that homochiral *cis*-ACPC homoligomers attain a nonpolar-strand conformation,[14a] whereas the alternating heterochiral *cis*-ACPC sequence stabilizes the H10/12 helix. These results indicate that the set of cyclic β-amino acid diastereomers is a complete toolbox, which allows the design of any major type of the β-peptide secondary structures.[21] As concerns the H10/12 helix, the constrained side-chain stabilization technique can be introduced, which may be beneficial for future biological applications. The relationship observed between the backbone chirality pattern and the preferred secondary structures can contribute to the principles of the rational β-peptide foldamer design and to the developing field of β-peptide self-assembling systems.

Experimental Methods

Peptide Synthesis. The synthesized ACPC-containing oligomers were as follows: (H-[(1*S*,2*R*)-ACPC-(1*R*,2*S*)-ACPC]$_2$-NH$_2$) (**1**), (H-[(1*S*,2*R*)-ACPC-(1*R*,2*S*)-ACPC]$_3$-NH$_2$) (**2**), (H-[(1*S*,2*S*)-ACPC-(1*R*,2*R*)-ACPC]$_2$-NH$_2$) (**3**), and (H-[(1*S*,2*S*)-ACPC-(1*R*,2*R*)-ACPC]$_3$-NH$_2$) (**4**). The sequences were synthesized by a solid-phase technique, utilizing *t*Boc chemistry.[22] The peptide chains were elongated on a *p*-methylbenzhydrylamine resin (0.63 mmol/g), and the syntheses were carried out manually on a 0.25 mmol scale. Couplings were performed with 3 equiv of dicyclohexylcarbodiimide and hydroxybenzotriazole, generally without difficulties. For **4**, after the fourth residue, the coupling step became difficult; during the monitoring of the coupling steps, the amount of truncated sequences increased. This is in accord with the observed association propensity, which possibly took place on the resin too. The amino acid incorporation was monitored by means of the ninhydrin test[23] and by the cleavage of aliquots from the resin. The peptide sequences were cleaved from the resin with liquid HF/dimethyl sulfide/*p*-cresol/*p*-thiocresol (86:6:4:2, v/v) at 0 °C for 1 h. The HF was removed, and the resulting free peptides were solubilized in 10% aqueous acetic acid, filtered, and lyophilized. Crude peptides were purified by reverse-phase HPLC, using a Nucleosil C-18 7 μ column (16 mm × 250 mm). The HPLC apparatus was made by Knauer (Berlin, Germany). The solvent system used was as follows: 0.1% trifluoroacetic acid (TFA) in water, 0.1% TFA, 80% acetonitrile in water; the gradient was 0% → 25% B during 15 min, then 25% → 55% during 60 min, at a flow rate of 3.5 mL/min, with detection at 206 nm. The appropriate fractions were pooled and lyophilized. The purified peptides were characterized by mass spectrometry, using a Finnigan TSQ 7000 tandem quadrupole mass spectrometer equipped with an electrospray ion source. The measured (calculated) molecular weights were as follows: 462.1 (461.62), 684.3 (683.99), 462.2 (461.62), and 684.3 (683.99) for **1**, **2**, **3**, and **4**, respectively.

NMR Experiments. NMR measurements were performed on Bruker *Avance* DRX 400 and 600 MHz spectrometers with a multinuclear probe with a *z*-gradient coil in 8 mM CD_3OD, DMSO, and water solutions at 303.1 K. The ROESY measurements were performed with a WATERGATE solvent suppression scheme. For the ROESY spinlock, 225 and 400 ms mixing times were used; the number of scans was 64. The TOCSY measurements were performed with homonuclear Hart-

(21) Fülöp, F.; Martinek, T. A.; Tóth, G. K. *Chem. Soc. Rev.* **2006**, *35*, 323−334.
(22) Merrifield, R. B. *J. Am. Chem. Soc.* **1963**, *85*, 2149−2154.
(23) Kaiser, E.; Colescott, R. L.; Bossinger C. D.; Cook, P. *J. Anal. Biochem.* **1970**, *34*, 595−598.

man−Hahn transfer with the MLEV17 sequence, with an 80 ms mixing time; the number of scans was 32. For all the 2D spectra, 2024 time domain points and 512 increments were applied. The processing was carried out by using a cosine-bell window function, with single zero filling and automatic baseline correction.

VCD Experiments: VCD spectra at a resolution of 4 cm^{-1} were recorded in DCM and DMSO-d_6 solution with a Bruker PMA 37 VCD/PM-IRRAS module connected to an Equinox 55 FTIR spectrometer. The ZnSe photoelastic modulator of the instrument was set to 1600 cm^{-1}, and an optical filter with a transmission range of 1960−1250 cm^{-1} was used in order to increase the sensitivity in the carbonyl region. The instrument was calibrated for VCD intensity with a CdS multiple-wave plate. A CaF_2 cell with a path length of 0.207 mm and a sample concentration of 10 mg/mL were used. VCD spectra were obtained as averages of 21 000 scans, corresponding to a measurement time of 6 h. Baseline correction was achieved by subtracting the spectrum of the solvent obtained under the same conditions.

CD Measurements. CD spectra were measured on a Jasco J810 dichrograph at 25 °C in a 0.02 cm cell. Eight spectra were accumulated for each sample. The baseline spectum recorded with the solvent only was subtracted from the raw data. The concentration of the sample solutions was 4 mM in CD_3OH and 1 mM in water. The data were normalized for the number of chromophores.

TEM Measurements. Droplets of 10 μL of solutions were placed onto the specimen holder, a carbon-film-coated 400 mesh copper grid (Electron Microscopy Sciences, Washington DC). First, the solution of the aggregated sample was applied to the grid and incubated for 2 min, while the particles accessed the specimen support by Brownian motion and adhered to it. The specimens were then optionally fixed with 0.5% (v/v) glutaraldehyde solution (for 1 min), washed three times with double-distilled water, and finally stained with 2% (w/v) uranyl acetate (by incubation of 2 min). Excess of solution was removed by suction with a filter paper attached to the edge of the grid, leaving behind a thin film of solution, which dried rapidly. After this evaporation, the uranyl acetate crystallites covered the object as a thin, amorphous coating. Because of the higher scattering power of the surrounding staining material, the aggregates appeared as structured light areas against a darker background when viewed in the TEM (negative staining).

Specimens were studied with a Philips CM 10 transmission electron microscope (FEI Company, Hillsboro, Oregon) operating at 100 kV. Images were taken with a Megaview II Soft Imaging System, routinely at magnifications of ×25000, ×46000 and ×64000, and analyzed with an AnalySis 3.2 software package (Soft Imaging System GmbH, Münster, Germany).

Molecular Mechanics Calculations. Molecular mechanical simulations were carried out on an HP workstation xw6000 in the Chemical Computing Group's Molecular Operating Environment. For the energy calculations, the MMFF94x force field was used, with a 15 Å cutoff for van der Waals and Coulomb interactions. Before the restrained simulated annealing (RSA), a random structure set of 100 molecules was generated by saving the conformations during a 100 ps dynamics simulation at 1000 K every 1000 steps. The RSA was performed for each structure with an exponential temperature profile in 75 steps, and a total duration of 25 ps, and the H-bond restraints were applied as a 10 kcal/(mol/$Å^2$) penalty function. Minimization was applied after every RSA in a cascade manner, using the steepest-descent, conjugate gradient, and truncated Newton algorithm.

Ab Initio Calculations. The molecular structure, stereochemistry, and geometry of the ACPC oligomers were exclusively defined in terms of their *z*-matrix internal coordinate system. The optimizations were carried out in two steps with the Gaussian 03 program: first by using the HF/3-21G basis set, and second, by using density-functional theory at the B3LYP/6-311G** level with a default setup. The theoretical VCD spectrum of **2** was calculated with the Gaussian 03 program at the B3LYP/6-31G* level of theory, for a geometry optimized in a vacuum at the same level. The calculated vibrational frequencies were scaled by a factor of 0.963. VCD curves were simulated from the calculated wavenumber and rotatory strength data by using Lorentzian band shape and a half-width at half-height value of 6 cm^{-1}.

Acknowledgment. We thank the Hungarian Research Foundation (OTKA No. T047186 to E.V. and T049792 to M.H.) and the National Research and Development Office, Hungary (OMFB-0066/2005-DNT, GVOP-311-2004-05-0255/3.0 and GVOP-3.2.1-2004-04-0345/3.0) for financial support. The computational resources of HPC U-Szeged (ALAP4-00092/2005) is acknowledged. T.A.M. acknowledges the award of a János Bolyai scholarship from the Hungarian Academy of Sciences.

Supporting Information Available: Signal assignments in CD_3OH and DMSO-d_6, ROESY, and TOCSY spectra recorded in DMSO, coordinates and energies of the ab initio structures, and complete ref 16. This material is available free of charge via the Internet at http://pubs.acs.org.

JA063890C